Excited state of protonated benzene and toluene

Natalia Esteves-López, Claude Dedonder-Lardeux, Christophe Jouvet

Excited state of protonated benzene and toluene

Natalia Esteves-López, Claude Dedonder-Lardeux, Christophe Jouvet*

Aix-Marseille Université, CNRS, UMR-7345, Physique des Interactions Ioniques et Moléculaires (PIIM). Marseille, France

*Corresponding author: Christophe.jouvet@univ-amu.fr

Abstract

We present photo-fragmentation electronic spectra of the simplest protonated aromatic molecules, protonated benzene and toluene, recorded under medium resolution conditions and compared with the photo-fragmentation spectrum of protonated pyridine. Despite the resolution and cold temperature achieved in the experiment, the electronic spectra of protonated benzene and toluene are structure-less, thus intrinsically broadened. This is in agreement with the large geometrical changes and the fast dynamic toward internal conversion predicted by ab-initio calculations for protonated benzene (M. F. Rode, A. L. Sobolewski, C. Dedonder, C. Jouvet, and O. Dopfer, J. Phys. Chem. A **113**, 5865–5873 (2009).

Introduction

The characterization of the structure, dynamics, and electronic properties of protonated molecules, mainly organic molecules, is of fundamental interest in physical and organic chemistry. Protonated aromatic molecules play a key role as short-lived intermediates in a broad range of environments, such as astrochemistry, jet engine gas exhaust or various hydrocarbon plasmas. Very few gas phase electronic spectra[1–3] of protonated aromatic ions were known until these last five years, but since then many experimental teams have been working on this subject[4–10].

The simplest protonated aromatic molecule, benzene, has not been characterized at high resolution. The information about the electronically excited states of $C_6H_7^+$ is available from early UV absorption spectra in solution[11] and from a low-resolution (10 nm) UV photo-dissociation spectrum of $C_6H_7^+$ isolated in an ion cyclotron resonance mass spectrometer. The gas-phase spectrum shows two electronic transitions at 330 and 245 nm[1,3] and deviates significantly from the solution spectrum in which the lower band is around 440 nm illustrating the drastic impact of the surrounding on the optical properties of protonated benzene. Recently the $C_6H_7^+$ spectra have been revisited in neon matrix by Garkusha *et al.*[12] One band

at 325 nm has been assigned to the $A^1B_2 \leftarrow X^1A_1$ transition of protonated benzene and no vibrational structure was observed possibly due to the interaction with the matrix.

Previous quantum chemical calculations[13] agree that the benzenium ion (σ complex, C2v symmetry) is the global minimum on the potential energy surface in the ground electronic state of $C_6H_7^+$ [14,15,16]. Excited state optimizations were performed by Rode et al. [13] at the ri-CC2, TD-DFT and CASPT2 levels, using the cc-pVTZ basis set and starting from the C2v ground state geometry. These excited state optimizations lead to barrier free ring deformation for the first four states. The ππ* states (S_1 and S_3) will decay in a barrier less manner through a conical intersection with the ground state via out-of-plane deformations of the ring. The σπ* states (S2 and S4) decay through a conical intersection with the ππ* states via an in-plane ring deformation. Thus on the basis of ab initio calculations, none of the first four excited singlet states of protonated benzene should show any measurable fluorescence but should undergo a fast non-radiative decay, probably on the femtosecond time scale.

This prediction cannot be tested from the only available spectrum due to its low resolution[3], and indeed the vibrational structure of protonated pyridine is not observed under the same experimental conditions whereas the vibronic levels can be clearly observed when cold ions are excited with our medium optical resolution (vide infra).

In this paper, we present the photo-fragmentation spectrum of cold protonated benzene, which shows that indeed the spectrum is structure-less indicating strong geometrical deformation in the excited states and/or a very short excited state lifetime. For comparison the electronic spectra of two other protonated molecules are presented, toluene which is similar to benzene, and pyridine.

Methodology

The experimental setup has been modified from the setup described previously[17] and is depicted below.

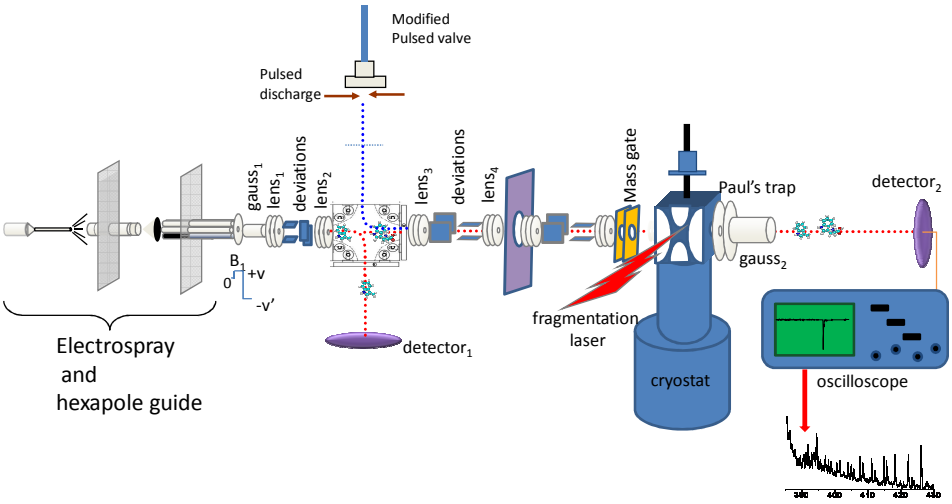

Figure 1: Scheme of the experimental setup.

It consists of an ion source, a Paul trap cryogenically cooled (30 K) and a time of flight mass spectrometer to analyze the fragments issued from the fragmentation of the ions excited in the trap by an OPO laser. Protonated benzene cannot be easily produced with the electrospray source, so we have added in the setup a discharge source similar to the one used previously for the study of protonated PAHs[18]. Thus the experiment can work with an electrospray source or a discharge source.

The electrospray ion source is composed of a needle (3000 V) injecting a solution of the molecule under study in methanol 50%/water 50% in a heated capillary. The ion beam produced is skimmed, injected in an octopole ion guide and extracted with a pulsed electrode to make ion bunches.

The discharge at the exit of a pulsed valve is the same as previously used in ref 18, the selection between the sources is realized by an ion bender. The deflector can also be used to direct the ions to detector$_1$ (see Figure 1) to check the stability of the ion source.

The ion bunches are guided with electrostatic lenses and deviation electrodes towards a mass filter, where the ions under study are mass selected by their time of flight. The ions are then trapped in a Paul trap cooled by a cryostat and filled with helium buffer gas. The ions are cooled by collisions while they stay in the trap. After some time (a few milliseconds) a laser is triggered to fragment the cold ions. The fragment and remaining parent ions are then ejected

in a time of flight mass spectrometer and detected on microchannel plates. The signal is send to an oscilloscope interfaced with a computer.

The OPO laser (EKSPLA NT342B), which has a resolution of around 8 cm^{-1} (0.1 nm), is scanned by step of 0.1 nm for fast scans and 0 .02 nm near the band origins.

The temperature of the ion in the trap is not necessary the same as measured by the temperature sensors located on the trap itself: the sensor located near the cryostat head measures 12 K and the other one located on top of the trap measures 35 K. More information can be obtained using Franck-Condon simulations for a molecule in which the calculated spectrum is in good agreement with the experimental one. This is the case of protonated acridine for which the intensity of the hot band indicates a temperature of 40±10K (see Figure S1 in Supplementary Information[19]). We have also checked on protonated pyridine that the ions kept in the trap for 80 ms before laser excitation are as cold when they are coming from the discharge as when they come from the electrospray source (see inset of Figure 2b).

The discharge source does not produce only protonated species, but a mixture of radical cations M^+ and protonated molecules MH^+, which are both trapped and cooled down. The mass selection that we can achieve with the setup is not sufficient to select only the MH^+ ion. So for benzene, the spectrum recorded on the fragment ion signal (m/z=77) corresponds to the loss of H from benzene cations $C_6H_6^+$ and the loss of H_2 from protonated benzene $C_6H_7^+$. However the electronic bands can be assigned in comparison with the parent ion depopulation.

In the case of toluene we have a similar problem since the discharge is producing m/z=91 (benzylium, $C_7H_7^+$), 92 (toluene ions $C_7H_8^+$) and 93 (protonated toluene, $C_7H_9^+$). As for benzene the assignment can be obtained by correlation between the fragment population and parent ion depopulation.

Results/discussion

Protonated benzene

The photofragmentation spectrum of protonated benzene is presented in Figure 2a, in comparison with the photofragmentation spectrum of protonated pyridine (Figure 2b). For this latter spectrum the ions are issued from the electrospray source, but it can be seen in the inset that the spectra obtained using either the discharge source or the ESI are identical. This spectrum is very similar to the one recently published[20], but it is at lower temperature so that no hot bands are observed. This spectrum shows that vibrational progressions can easily be

observed in our apparatus and these progressions have already been assigned by Hansen *et al.*[20]

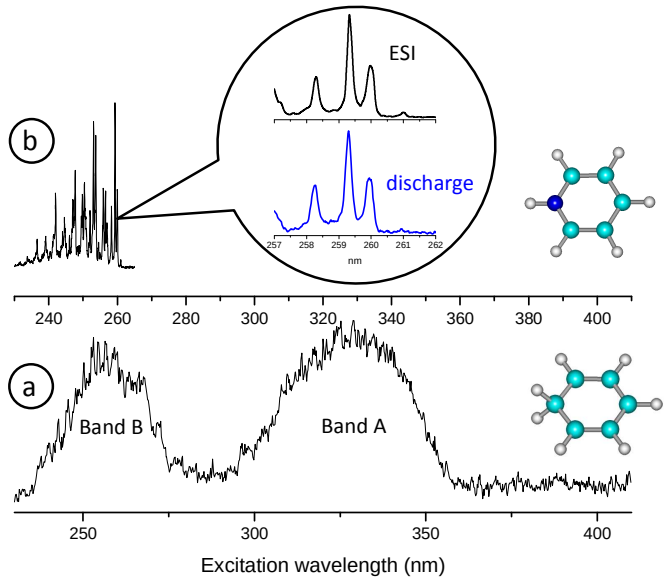

Figure 2: **a) photofragmentation spectrum of protonated benzene BH^+ and benzene cation B^+ recorded on the m/z=77 fragment mass ($C_6H_5^+$). The first band A, which is due to BH^+ only, is totally structure-less. The second band B is due to the photofragmentation of both B^+ and BH^+ (see supplementary information). The "structures" observed in the 250 nm region are due to large variations of the laser intensity, which are not completely corrected. b) photofragmentation spectrum of pyridineH^+. The spectrum is well structured showing that the vibrational bands are easily observed when present. In the inset part of the spectra obtained from fragmentation of protonated pyridine produced by the discharge source (lower blue trace) and by the electrospray source (upper black trace). Within the experimental error both spectra are identical.**

The protonated benzene photofragmentation spectrum presents two broad bands: band A starting at 360 nm and centered at 325 nm (3.81 eV) and band B starting around 280 nm and centered at 255 nm (4.86 eV).

For protonated benzene, the only fragment corresponds to the loss of H_2 (fragment ion m/z 77) as observed by Freiser *et al* [3]. Loss of H_2 is the lowest energy dissociation channel for the protonated benzene $C_6H_7^+$ ions and the barrier-less dissociation to H_2 + $C_6H_5^+$ is reported to require 3.07 eV [21]. The discharge source is not producing only protonated species, but benzene radical cations ($C_6H_6^+$) are also trapped. For band A, we observe simultaneously the appearance of the m/z 77 fragment and the depopulation of the m/z 79 parent ion (protonated benzene), whereas the m/z 78 ion signal stays constant (see SI). Thus one can insure that

spectrum observed at m/z 77 corresponds to the photofragmentation of protonated benzene. At the opposite, band B is observed in the depopulation of $C_6H_6^+$ and weakly in the depopulation of $C_6H_7^+$.

The spectrum is very similar to the one obtained at low resolution and the two bands have already been assigned[13] to the $A^1B_2 \leftarrow X^1A_1$ transition for the A band, and to the $2^1A_1 \leftarrow X^1A_1$ transition for band B. The calculated oscillator strength is weaker for the second band (0.1 instead of 0.14) but part of the intensity is due to the absorption of the B^+ cation through the $^2E_{2u} \leftarrow ^2E_{1g}$ transition as observed by Freiser and Beauchamp[2], which is superimposed on the protonated benzene $2^1A_1 \leftarrow X^1A_1$ transition (see Figure S2 in the supplementary information)[19].

The most important observation is that the spectrum of the first excited state is intrinsically broad and structure-less. Since the resolution of the laser is 8 cm^{-1} (0.001 eV) and the ions are cold, only two factors contribute to the width of the experimental transitions (around 0.47 eV) observed at 325 and 255 nm, lifetime broadening and spectral congestion arising from large geometry changes. In the case of protonated pyridine (Figure 2) and acridine (Figure S1 in the supplementary information), the linewidth is around 10-12 cm^{-1}, which accounts for the convolution of the rotational contour by the laser width. We have also observed, in the case of protonated DNA bases[22], that excited state lifetime of the initially excited state can be estimated from the linewidth of the vibrational bands, in the order of 100 cm^{-1}, which corresponds to a lifetime of 50 fs. In the case of protonated benzene, calculations predict a large change in geometry between ground and excited states, without local minima in C2v geometry, which means that excitation will lead to a region of spectral congestion. Besides, calculations also predict conical intersections between the excited and ground states, which should lead to fast internal conversion and thus possibly to lifetime broadening. The absence of structure observed here is the combination of spectral congestion and lifetime broadening.

The difference between benzene and protonated DNA bases is illustrated in Figure 3. For a nearly flat potential surface in planar geometry, we would have observed broadened vibrations as in the case of protonated DNA bases (Figure 3, left). In a diabatic point of view, such a surface results from a weak coupling between two states ($\pi\pi^*$ and $n\pi^*$), mostly due to vibronic coupling. The absence of vibrational structure in protonated benzene implies that there is no local minimum near the Franck Condon window i.e. for a C_2v geometry (Figure 3, right).

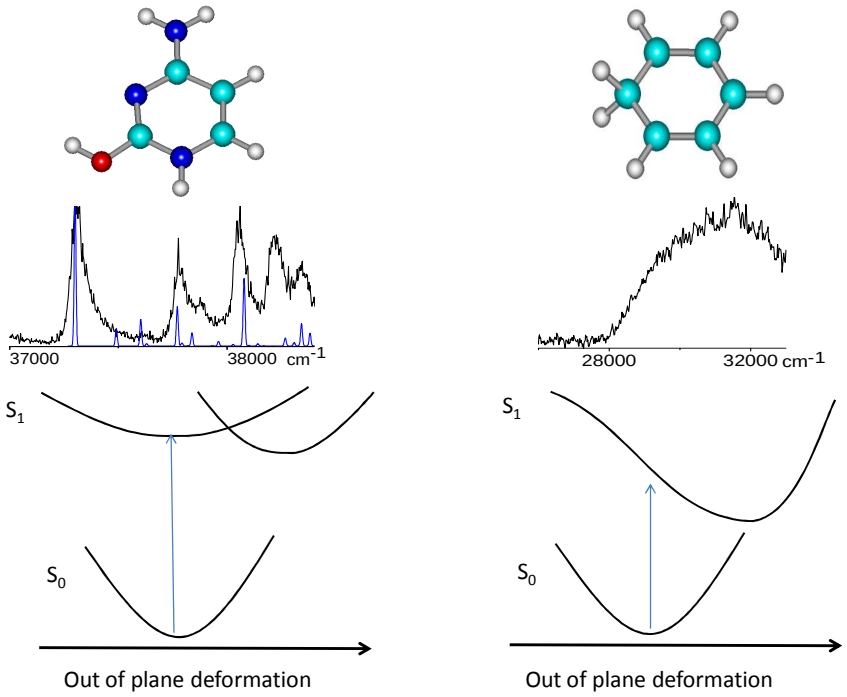

Figure 3: Upper part: comparison of the spectra of protonated thymine (Reproduced from Ref. 22 with permission from the PCCP Owner Societies) and benzene. For protonated thymine the calculated spectrum (in blue) shows that the broadening is not coming from low frequency modes. Lower part: scheme of the potential energy functions that can lead to the observed spectra for both systems

In any case these experimental results show that upon optical excitation the excited state has very different equilibrium geometry than the ground state. This is what was expected from *ab initio* calculations but needed to be demonstrated experimentally. Femtosecond experiments would be necessary to measure the excited state lifetime.

Protonated toluene

The ground state IR spectroscopy of toluene has been extensively studied by Dopfer *et al.* [23] through Infrared Red Multi Photon dissociation (IRMPD). Two tautomers (protonation in ortho and para position) are potentially observed in a room temperature ion trap. The ortho tautomer, which has a calculated ground state energy 5.6 kJ/mol (0.058 eV) higher than the para tautomer, fits better with the experimental IR spectrum. We did similar calculations at the (DFT/B3LYP/cc-pVQZ) level and found quite similar result (the ortho tautomer is calculated 5.7 kJ/mol higher in energy than the para tautomer). We have also calculated the excited states of both tautomers. The vertical S_1-S_0 transition of the para tautomer is at 4.24 eV (oscillator strength 0.10) while for the ortho tautomer the transition is calculated at 3.90 eV (oscillator strength 0.16) i.e. red shifted by 0.34 eV, so the transitions should be well

separated. As in protonated benzene, for both tautomers the excited state optimization leads to strong out of plane deformations resulting in a half chair type geometry for which the S_1 and S_0 states are degenerate. Thus, as for protonated benzene, a fast electronic relaxation is expected.

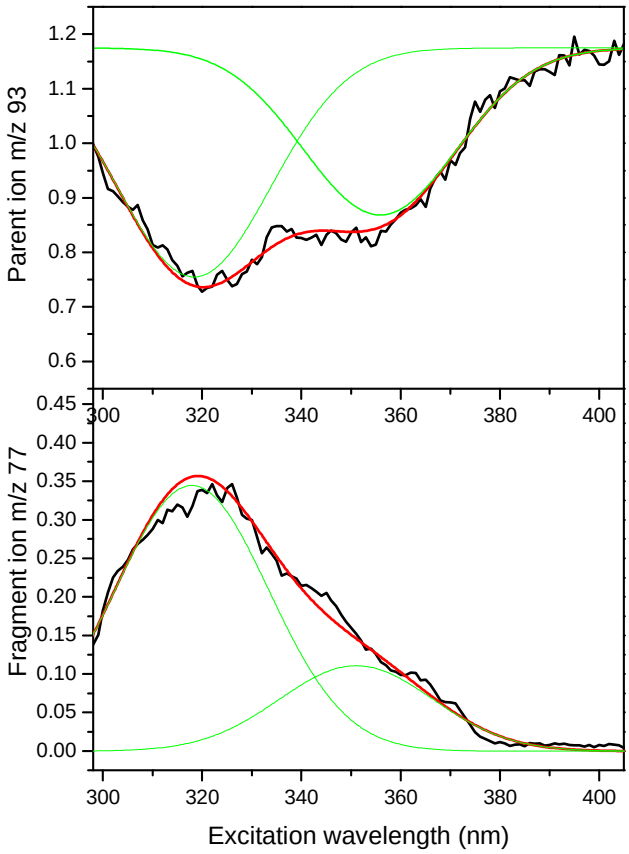

Figure 4: Photofragmentation spectra of protonated toluene: depopulation of the m/z=93 parent ion (upper trace) and population of the fragment ion at m/z=77 (lower trace). The intensity ratio between the 2 bands is not exactly the same between the two spectra since around 320 the m/z=77 fragment can also be produced by protonated benzene, which is an impurity produced by the discharge (see figure S3)[19].

Experimentally the broad spectrum observed in both the main dissociation product (m/z=77 CH_4 loss) and the depopulation of the protonated toluene (m/z=93), presents two contributions (figure 4). From *ab initio* calculations, the first band at 353 nm (3.51eV) can be assigned to the ortho tautomer and the second band peaking at 320 nm (3.87 eV) to the protonation in para position. The spectral shift between the two bands is 0.36 eV in agreement with the calculated vertical transition energies and the absolute values are within +0.5 ± 0.2 eV, as observed in previous work[22]. This means that despite the cold temperature obtained in

the ion trap (around 40 K) the equilibrium between the tautomeric forms is not achieved. This was already observed for protonated indole[17].

Conclusions

It is not clear what is controlling the non-radiative processes in protonated aromatic species. Very well structured spectra are observed for σ complexes in naphthalene[24,25] and indole[17] or larger aromatic molecules[18,26,27] whereas broad spectra are also observed for aminophenol protonated on the aromatic ring[28]. *Ab initio* calculations, predict strong changes in geometry between the ground and the excited state due to out of plane deformations of the benzene ring, which lead to a conical intersection with the ground state. Such ring deformations are also necessary to explain the very short excited lifetime of the protonated DNA bases, but in this latter case some lifetime broadened vibrational structures are still observed.

Acknowledgements

This works was supported the ANR Research Grant (ANR2010 BLANC040501). We acknowledge the use of the computing facility cluster GMPCS of the LUMAT federation (FR LUMAT 2764).

References

[1] B.S. Freiser and J.L. Beauchamp, J. Am. Chem. Soc. **98**, 3136 (1976).

[2] B.S. Freiser and J.L. Beauchamp, Chem. Phys. Lett. **35**, 35 (1975).

[3] B.S. Freiser and J.L. Beauchamp, J. Am. Chem. Soc. **99**, 3214 (1977).

[4] I. Alata, R. Omidyan, C. Dedonder-Lardeux, M. Broquier, and C. Jouvet, Phys. Chem. Chem. Phys. **11**, 11479 (2009).

[5] A. Patzer, M. Zimmermann, I. Alata, C. Jouvet, and O. Dopfer, J. Phys. Chem. A **114**, 12600 (2010).

[6] O. V Boyarkin, S.R. Mercier, A. Kamariotis, and T.R. Rizzo, J. Am. Chem. Soc. **128**, 2816 (2006).

[7] T.R. Rizzo, J. A. Stearns, and O. V Boyarkin, Int. Rev. Phys. Chem. **28**, 481 (2009).

[8] D. Nolting, C. Marian, and R. Weinkauf, Phys. Chem. Chem. Phys. **6**, 2633 (2004).

[9] S.Ø. Pedersen, C.S. Byskov, F. Turecek, and S. Brøndsted Nielsen, J. Phys. Chem. A **118**, 4256 (2014).

[10] S.B. Nielsen and J. Wyer, editors , *Physical Chemistry in Action:Photophysics of Ionic Biochromophores.* (Springer-Verlag Berlin Heidelberg, 2013).

[11] H.H. Perkampus and E. Baumgarten, Angew. Chem., Int. Ed. **3**, 776 (1964).

[12] I. Garkusha, J. Fulara, A. Nagy, and J.P. Maier, J. Am. Chem. Soc. **132**, 14979 (2010).

[13] M. Rode, A.L. Sobolewski, C. Dedonder, C. Jouvet, and O. Dopfer, J. Phys. Chem. A **113**, 5865 (2009).

[14] N. Solcà and O. Dopfer, Angew. Chemie Int. Ed. **41**, 3628 (2002).

[15] G.E. Douberly, A.M. Ricks, P. v. R. Schleyer, and M.A. Duncan, J. Phys. Chem. A **112** , 4869 (2008).

[16] W. Jones, P. Boissel, B. Chiavarino, M.E. Crestoni, S. Fornarini, J. Lemaire, and P. Maitre, Angew. Chemie - Int. Ed. **42**, 2057 (2003).

[17] I. Alata, J. Bert, M. Broquier, C. Dedonder, G. Feraud, G. Grégoire, S. Soorkia, E. Marceca, and C. Jouvet, J. Phys. Chem. A **117**, 4420 (2013).

[18] I. Alata, C. Dedonder, M. Broquier, E. Marceca, and C. Jouvet, J. Am. Chem. Soc. **132**, 17483 (2010).

[19]See Suppl. Mater. [URL Will Be Inser. by AIP] (n.d.).

[20] C.S. Hansen, S.J. Blanksby, N. Chalyavi, E.J. Bieske, J.R. Reimers, and A.J. Trevitt, J. Chem. Phys. **142**, 014301 (2015).

[21] E. del Rio, R. Lopez, and T.L. Sordo, J. Phys. Chem. A **101**, 10090 (1997).

[22] M. Berdakin, G. Féraud, C. Dedonder-Lardeux, C. Jouvet, and G.A. Pino, Phys. Chem. Chem. Phys. **16**, 10643 (2014).

[23] O. Dopfer, J. Lemaire, P. Maître, B. Chiavarino, M.E. Crestoni, and S. Fornarini, Int. J. Mass Spectrom. **249-250**, 149 (2006).

[24] I. Alata, M. Broquier, C. Dedonder-Lardeux, C. Jouvet, M. Kim, W.Y. Sohn, S. Kim, H. Kang, M. Schütz, A. Patzer, and O. Dopfer, J. Chem. Phys. **134**, 074307 (2011).

[25] I. Alata, R. Omidyan, M. Broquier, C. Dedonder, O. Dopfer, and C. Jouvet, Phys. Chem. Chem. Phys. **12**, 14456 (2010).

[26] I. Garkusha, J. Fulara, P.J. Sarre, and J.P. Maier, J. Phys. Chem. A (2011).

[27] J.A. Noble, C. Dedonder, and C. Jouvet, Astron. Astrophys. **A79**, 577 (2015).

[28] G. Féraud, N. Esteves-López, C. Dedonder-Lardeux, and C. Jouvet, Phys. Chem. Chem. Phys. (2015).